Global NEST Journal, Vol 25, No 5, pp 153-161

Removal of phenol from olive mill wastewater using activated rice husk

Wedian F.[1*], Al-Zboon K.[2], Mohamad S.[1,3] and Tashtoush R.[4]
[1]Department of Chemistry, Faculty of Science, Yarmouk University, P.O. Box 560, Irbid 22163, Jordan
[2]Environmental Engineering Department, Al-Balqa Applied University, P.O. Box 50, 21510, Jordan
[3]Applied Science Department, Huson, Jordan, Al-Balqa Applied University, P.O. Box 50, 21510, Jordan
[4]Chemical Engineering Department, Huson, Jordan, Al-Balqa Applied University, P.O. Box 50, 21510 Huson, Jordan
Received: 22/11/2022, Accepted: 05/01/2023, Available online: 01/03/2023
*to whom all correspondence should be addressed: e-mail: alwedian@yu.edu.jo
https://doi.org/10.30955/gnj.004583

Graphical abstract

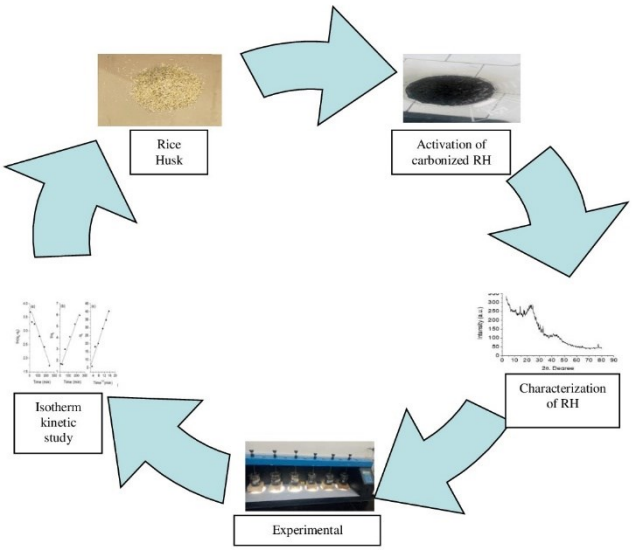

Abstract

Olive mill wastewater (OMWW) contains many phenolic compounds that if discharged without proper treatment, may lead to substantial risks to human health and deterioration of the environment and aquatic systems. In this study, an attempt was made to produce activated carbon from Rice Husk (RH). The RH was chemically activated by calcium chloride and was utilized for the removal of phenol from the aqueous solution. The removal efficiency using the Activated Rice Husk (ARH) was investigated at different variables such as pH, contact time, adsorbent dose, initial concentration, and carbonization temperature. Results showed that the optimum removal efficiency was 91.62% which was achieved at pH=6, carbonization temperature=850 ˚C, and after 4hrs contact time. Adsorption isotherm fitted well to Langmuir and Freundlich isotherm models while the kinetic data fitted well to the pseudo-second-order model, and thermodynamic data showed that the adsorption is endothermic in nature. Then the activated rice husk sample was used for phenol removal from real OMWW samples from different locations in the city of Irbid-Jordan providing average removal efficiency reached 94.6%. The study indicates that RH and ARH have good potential to be used for phenol removal.

Keywords: Olive mill wastewater, rice husk, phenol, adsorption, activated rice husk

1. Introduction

Olive oil production is a powerful for human diet and health because it is a resource ofantioxidant agents and essential fatty acids, so olive oil production has been increased in the Mediterranean as a wariness of its health and economic benefits is raised. Olive oil is produced through pressing process of olive fruits using either; traditional pressing or continuous centrifugation method (Rahmanian, 2014). Both methods yield 3 phases streams; solid, oily, and aqueous residues, which generate solids and aqueous waste.

Wastewater from olive mill is an acidic liquid waste generated as aside-stream from olive oil production. This waste consists of liquid oil and water and solids materials (Niaounakis *et al.*, 2006). Methods of olive oil pressing have negative impact on the environment because large amount of olive mill waste is produced during a short period pose heavy environmental load. The high content of phenol in waste causes serious impacts on the environment and the ecosystem.

Phenol compound is a hydroxyl group bonded to benzene ring; it has molecular formula C_6H_5OH and has white solid crystals. Unite States Environmental Protection Agency (US EPA) designates phenol as 11th of the 126 chemicals, which as priority pollutants (Dursun *et al.*, 2005). Discharge of such hazardous material without required treatment may lead to substantial risks to human health and deterioration of the environment and aquatic system, phenol is a highly toxic compound that requires removal, even if it is found in low concentration, has effect on soil, water, atmosphere, aquatic life, and genotoxicity by release of heavy metals and number of microbes increased in soil, reduce the solubility of oxygen in water, due to high content of

reduced sugar that microorganism used as a substrate in OMWW, If an open tank is used to store OMWW, fermentation and emission of gases will be occurred, ability to biodegradation of tannins, without biodegradation of phenol, and the high content of phenol in OMWW has genotoxic effected on the human and animal cell (Michalowicz, 2006).

Different methods have been used for phenol removal from (OMWW) such as biologicaltreatment, evaporation, solvent extraction, Fenton reaction, and adsorption. Biological treatment is a time consuming, and it is not recognized as a valorization technique, evaporation comes with additional problems associated with the remaining concentrate and needs additional treatment. Solvent extraction methods lead to large quantities of waste and toxic compounds. Fenton reaction method is more combined since it implicates numerous additional reactions (DellaGreca *et al.*, 2001).

Adsorption is a powerful technique for treatment (OMWW). It occurs when a molecule transfers from aqueous phase to solid phase due to chemical bond or physical force (Artioli, 2008). The adsorption offers some advantages such as cost effectiveness and energy efficiency (Al-Zboon *et al.*, 2019). Recycling the waste is a good process for reducing the negative impact of waste on the environment and for reducing the cost of waste management (Al-Zboon *et al.*, 2019). Any activated carbon substance with a high surface area and high pore volume can be a good adsorbent for removal (Abe and Otsuka, 2012). The activated carbon generated from RH is utilized as a superior adsorbent for removal of phenol from (OMWW). Cellulose (32%), hemicelluloses (20%), lignin (21%), and other organic materials (20%), including protein and fat, make up many of the chemical components of RH. There are numerous methods for physically and chemically activation of carbon. Physical activation results in a small surface area while chemical activation produces a larger output of carbon and lower cost. With chemical agents like NaOH, $CaCl_2$, H_3PO_4, KOH, and others, chemical activation occurs at high temperatures. Many researches and methods have been conducted to enhance and modify the surface of activated carbon by adding specific functional (acidic or basic) group, to increase pore size and surface area, and subsequently increases its capacity for adsorption. Using acidic functional groups such as lactone, carboxyl, hydroxyl, quinone and carboxylic anhydride has shown increasing the capacity of activated carbon (Yin *et al.*, 2007).

Over the years, numerous techniques have been employed to extract phenol from wastewater. The majority of these techniques are pricy, impractical, and chemically intensive (Toheed *et al.,* 2000). Many researchers investigated the efficiency of phenol removal by different materials: Sahua *et al.* (2017) found that the optimum adsorption capacity of phenol on saw dust was 78.3%. In a similar work, Sayed (2008) applied batch kinetic technique to remove phenol using Kaolina Mineral Clay and he achieved a percent of removal up to 100%. Infrared spectra, thermo gravimetric and differential thermal analysis technique were used to characterize kaolina clay with phenol. Using Iraq rice husk, Nasif *et al.* (2013) studied the effect of different parameters such as pH, initial concentration of phenol, treatment time, feed flow rate, and temperature on phenol removal from solution. They found that with lower phenol concentration (1 mg/l), the removal effectiveness increased to 89.73%. Asgharania *et al.* (2019) investigated the effect of initial concentration, pH, and dosage of adsorbent and contact time on phenol removal by ARH, as a low-cost adsorbent and achieved a percent of removal reached up to 91% at pH 6 after 120 minutes. Ghasemi *et al.* (2011) prepared AC from rice straw by physical and chemical treatments and used it for phenol removal they studied the effect of different parameters such as: different mass of adsorbent and different contact time and other parameters, the highest removal percentage reached 84%. Daffalla *et al.* (2010) developed low-cost RH to be a good adsorbent for phenol removal, chemical and thermal treatment was done to develop the surface area of RH; the adsorbent properties were characterized using FT-IR, SEM and FSEM. Functional groups such as (OH, Si-OH, Si-O-Si, O-CH_3) were increased on the surface of adsorbent, which indicated that the surface area increased and the maximum removal efficiency was up to 96.5%, which was obtained after 4hr of mixing.

This work aims are to produce activated rice husk using calcium chloride as activating agent and investigate the effect of various operating conditions such as pH, initial concentration, temperature of carbonization, dose and contact time that will affect phenol removal. Also, thermodynamic, kinetic and isotherm studies were conducted.

2. Materials and method

2.1. RH preparation

Rice husk was washed with distilled water to remove all impurities, and dried in an oven at 105 ˚C for 2hrs. After that, RH was placed in a ceramic crucible and carbonized in a muffle furnace (STUART-SCIENTIFIC) with absence of oxygen at different temperatures (400, 550, 700, 850°C) for 2hrs.

2.2. Chemical activation of RH

RH was chemically activated using ($CaCl_2$) to enhance the adsorption process and to increase the phenol removal. The chemical activation procedure involved immersing a 25.0 g of RH in 25% of $CaCl_2$ solution for 24 hrs. After that the resulting activated carbon was filtered, washed with distilled water, and dried in an oven at 105 °C for 1 hour (Zanella *et al.*, 2014).

2.3. Characterization of (ARH)

2.3.1. Specific surface area for ARH

The specific surface area of ARH can be calculated from the amount of the adsorbed methylene blue. It was reported that the occupied surface by one molecule of methylene blue is 130 $A^{\circ 2.}$ The equilibrium concentrations of methylene blue can be obtained from the calibration curve. Then the specific surface area for ARH was calculated by Eqn (1) (Pelekani *et al.*, 2000).

$$S_s = \frac{q_e \times N \times A_{MB}}{W} \quad (1)$$

Where S_s is specific surface area ($m^2\ g^{-1}$), qe is amount of methylene blue adsorbed (mg g^{-1}), W is a molar mass of methylene blue (319.86×10^3 mg mol^{-1}), N is Avogadro's number (molecule mol^{-1}), A_{MB} is area covered by one molecule of methylene blue (130×10^{-20} m^2).

2.3.2. Boehm titration

Boehm titration can be used to identify the surface of different acidic functional groups of ARH by titration them with different base strengths. The procedure of titration is as follows:

A 4.5 g of ARH was dried overnight at 120 ℃, 1.5 g of ARH was placed into three of 50 mL volumetric flasks. 20 mL of 0.05 M of NaOH, 20 mL of 0.05 M N_2CO_3 and 20 mL of 0.05 M $NaHCO_3$ were added to the flasks respectively. The mixtures were shaken for 24hrs, and then filtered to remove carbon by a 0.2 µm nylon-membrane syringe micro filter. Pipette 10 mL from three filtered solutions was transferred to three new flasks. The 10 mL of NaOH and $NaHCO_3$ solutions were acidified by the addition of 20 mL of 0.05 M HCl; the 10 mL of Na_2CO_3 was acidified with 30 mL of 0.05 M HCl. All acidified solutions were back-titration with standardized 0.05 M sodium hydroxide, under degassing with nitrogen gas for 2hrs to remove carbon dioxide. The equation used to determine the quantity of surface groups depends on the titration methods, the amounts of the acidic groups on the carbon surface are determined by Eqn. (2), (Goertzen *et al.*, 2010):

$$n_{s=}\frac{n_{HCl}}{n_B}[B]V_B - ([HCl]V_{HCl} - [NaOH]V_{NaOH})\frac{V_B}{V_a} \quad (2)$$

where B is the concentration of reaction base (M) V_B is the volume of reaction base (mL), n_s is the moles of carbon surface functional groups that reacted within base during mixing (mmol g^{-1}), V_a is the volume of the aliquot taken from base solution after filter carbon (mL), [HCl] is concentration the acid added to the aliquot taken from the original sample (M), V_{HCl} is the volume of acid added to the aliquot taken from the origin sample (mL), [NaOH] is the concentration of NaOH used as a titrant (M), V_{NaOH} is the volume of NaOH consumed in the titration (mL), n_{HCl}/n_B is a stoichiometric ratio of HCl to base.

2.3.3. Fourier transform spectroscopy

The surface functional group for ARH was performed using Fourier Transform Spectroscopy (FT-IR) from (Alpha-Bruker company, US).

2.3.4. X-Ray diffraction (XRD)

Prepared ARH (carbonized at 550 ˚C and immersed with 25% calcium chloride) has been analyzed using X-Ray copper with 40 KV, 30 mA of current (Shimadzu-XRD 6000) Ka gun (λ =1.541), the speed of scanning was 3.00 degree/minute.

2.3.5. Phenol adsorption

A stock solution of phenol was prepared by dissolving 1.1 g of phenol (85%, 94.11 g mol^{-1}, d=1.07 g/mL) in a 1 L distilled water to get 1000 mg^{-1}L. Working solution prepared by a series ofdilution to get four concentrations 25, 50, 75, 100, and 125 mg^{-1}L. The different concentrations of phenol were analyzed using a Shimazdu spectrophotometer1800 instrument at 270 nm wavelength to give a linear calibration curve.

2.3.6. Experimental conditions of the ARH Adsorption

The ARH adsorption capability was assessed at different experimental conditions in order to obtain the optimum conditions for removal efficiency. Removal efficiency was investigated at different pH (2, 3, 4 ,5, 6, 7, 8, 9, and 10), different ARH dosage (1, 2, 3, and 4 g carbonized at 550 ˚C), variable phenol concentrations (25, 50, 75, 100, and 125 mg^{-1} L), with different contact (mixing) time (10, 30, 60, 120 min) and four carbonization temperatures (400, 550, 700 and 850 ˚C).

3. Results and discussions

3.1. Characterization of ARH

3.1.1. Surface area of RH and ARH

Surface area for RH and ARH were calculated using MB method. The results of calculation showed that ARH has more surface area ($53m^{-2}$ g) than RH ($12.5m^{-2}$ g). This result proves the feasibility and effectiveness of the activation process. The activation process increased the surface area by more than 330%. Many researchers reported that activation process has positive effect in the surface area of RH, for example Liu *et al.* (2016) was found the surface area for ARH reached to 1924 m^{-2}g.

3.1.2. Boehm titration

The surface of activated carbon is rich with oxygen containing functional groups, to determine the acidic and basic groups, sodium hydroxide is used as strong base to neutralize all Bronsted acids groups (phenols, lactonic, carboxylic acids), while sodium carbonate neutralize lactonic groups and sodium bicarbonate neutralize carboxylic acids. The results of calculation of surface functional groups are listed in Table 1. The result showed that; phenolic, carboxylic, and lactonic groups contribute to the surface of ARH according to the value of n_s which means that the acidic and basic groups were found on the surface area of activated carbon and caused increasing in the pore size and surface area of ARH (see Table 1).

Table 1. Acidic functionalities determined by Boehm titration for rice husk activated with $CaCl_2$.

	ns (µmol g-1)		
	Phenolic	Lactonic	Carboxylic
ARH-CaCl2	220	40	140
Activated carbon "Abu Dalo (2017)"	188	155	158

3.1.3. Fourier transform infrared (FTIR) spectroscopic analysis

The surface functional groups of ARH-$CaCl_2$ were determined by FT-IR spectroscopy. Figure 1 shows the FT-IR spectra for ARH-$CaCl_2$. It was characterized by the presence of:

A band transmittance around 400 cm^{-1} is assigned as O-H stretching vibration of hydroxyl group. Another broadband was found at around 1632.1 cm^{-1} corresponding to C=O

stretching vibration in carboxyl groups aldehydes, ketones or lactones and associated to C=C stretching vibration in aromatic rings.

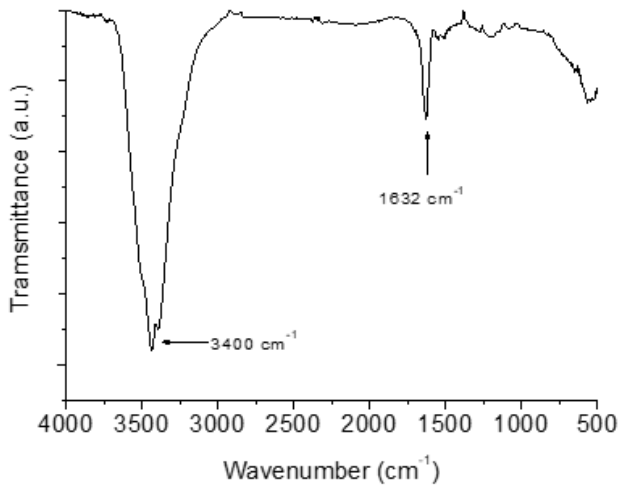

Figure 1 FTIR spectrum of rice husk activated with $CaCl_2$

3.1.4. X-Ray diffraction (XRD)

The diagram of XRD for ARH is shown in Figure 2. It indicates a broad peak due to amorphous carbon in the RH. (Wanyika *et al.*, 2011) explained that the wider the angle in XRD is a result of existence of a large porous in the tested materials (Kioni *et al.*, 2011).

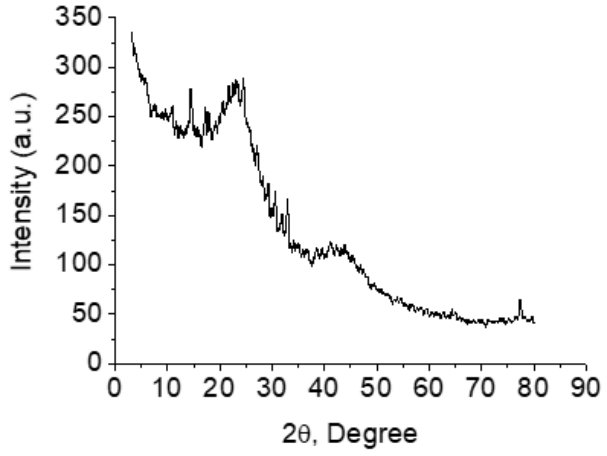

Figure 2 The X-ray diffraction of rice husk activated with $CaCl_2$

3.2. Adsorption studies

The concentration of phenol after adsorption was determined from the calibration curve of phenol, the percent of removal (%*R*) for all parameters can be calculated with the following Eqn. (3) and the adsorption capacity can be calculated using Eqn. (4) (Al-Zboon *et al.*, 2019) and (Al-Zboon *et al.*, 2017):

$$\%R = \frac{C_0 - C_e}{C_0} \times 100\% \quad (3)$$

$$q = \frac{C_0 - C_e}{m} \times V \quad (4)$$

where C_0 is the initial concentration of phenol (mg^{-1} L), C_e is the equilibrium concentration of phenol (mg^{-1} L), q is the amount of uptake phenol (mg^{-1} g), V is the volume of solution (Liters) and m is the mass of adsorbent.

3.2.1. Effect of solution pH

pH value is an important parameter that affects removal efficiency. Figure 3(a) indicates the removal efficiency increased with pH increase up to 6 and then decreased. The optimum removal efficiency was 58.8% at pH=6 for initial phenol concentration of 50 ppm, adsorbent dosage of 1g after 2h provided an adsorption capacity of 29.4 mg^{-1} g. This result is consistent with the work of (Kavitha *et al.*, 2016) and (Pajooheshfar *et al.*, 2009). At low pH values, there is an excess of H_3O^+ ions in the solution, which make a competition between the positively charged hydrogen ions (Al Zboon *et al.*, 2011) and this observation can be explained: at higher pH values, phenol ionizes then the affinity of phenol to water increases, and the electrostatic repulsion increases between phenol ion and the negatively charge surface of ARH, thus adsorption decreases (Lopez-Ramon *et al.*, 2009).

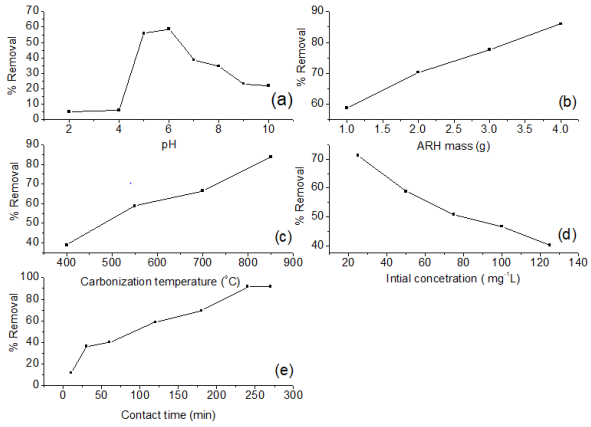

Figure 3 The effect of experimental condition on percent removal of phenol including: effect of (a) pH, (b) ARH mass, (c) carbonization temperature, (d) initial concentration, and (e) contact time

3.2.2. Effect of change ARH dose

The removal efficiency of ARH was evaluated at different amount used ARH. Figure 3(b) shows the effect of ARH dose on phenol removal, the removal efficiency increased significantly as ARH dosage increases. The removal efficiency increased from 58.8% to 86% as the dose increased from 1 to 4 g while adsorption capacity decreased from 29 to 10.75 for the same doses respectively. This result complies with the work of (Sarker and Fakhruddin, 2017), and (Asghjarnia *et al.*, 2019). This increase is explained by increase the available adsorption site and the surface area of ARH (Alzboon *et al.*, 2011).

3.2.3. Effect of carbonization temperature

The effect of carbonization temperature was investigated at four temperatures: 400, 550, 700, 850 ℃. Figure 3(c) indicates that as temperature of carbonization increased, the removal efficiency was also increased to 83.8% at 850. This result agrees with Daffalla *et al.* (2010), they found that removal efficiency increased as carbonization temperature increased. And at high temperature inside can

cause water vaporization and formation of micro-cavities thereby increases adsorption capacity (Alzboon *et al.*, 2011)

3.2.4. Effect of the initial concentrations of phenol

Dependence of removal efficiency of ARH on the concentrations of phenol was carried out at different initial concentrations. As shown in Figure 3(d), the increase in initial concentration of phenol from 25-125 mg^{-1} L, resulted in a decreasing ofremoval efficiency from 71.2 to 40.1%. In contrast, q_e increased from 17.8 to 50.2 mg^{-1}g. This is due to the decrease in the available active sites in ARH surfaces at higher concentrations and thus lowering the removal efficiency. Pirzadeh *et al.* (2016) reported similar results. This explained by increases the concentration of adsorbent then the available pores of adsorbent become insufficient to adsorb all adsorbent (Al-Zboon *et al.*, 2016).

3.2.5. Effect of contact time

Figure 3(e) shows that phenol removal increased as increasing in contact time form 11.8 % after 10m to 91.62 % after 4hr. The adsorption capacity increased from 5.9 m^{-2} g to 29.4 m^{-2} g for the same times respectively. Similar results were reported by (Daraei *et al.*, 2014) and (Alzboon *et al.*, 2015). The removal of phenol was increased due to an increase in the capacity of ARH and as time progressed, ARH began to absorb a greater amount of phenol (Nasif *et al.*, 2013).

3.3. Adsorption isotherms

Adsorption isotherm describes the amount of solute absorbed in a bulk of solution per unite weight of adsorbent at constant temperature. To describe the adsorption mechanism of phenol on ARH, the experimental adsorption data of phenol were modeled using the Langmuir, Freundlich, Dubinin-Radushkevich, and Temkin models.

Langmuir Adsorption Isotherm was developed to represent chemisorption and suggests that the adsorbent contains a constant number of identical active sites and each site can take one molecule (mono-layer coverage only), so adsorbed molecules can't interact with neighboring molecules (Dad *et al.*, 2012). The linearized equation of the Langmuir isotherm model is given in Eqn. (5):

$$\frac{1}{q_e} = \frac{1}{q_{max}} + \left(\frac{1}{q_{max} \times K_L}\right)\frac{1}{C_e} \quad (5)$$

where C_e is the concentration of adsorbate at equilibrium (mg L^{-1}). q_e is the amount of adsorbate adsorbed per gram of the adsorbent at equilibrium (mg g^{-1}). q_{max} is maximum monolayer adsorption capacity at equilibrium (mg g^{-1}). K_L is Langmuir isotherm constant (L mg^{-1}). The K_L and q_{max} values are calculated by plotting $1/q_e$ vs. $1/C_e$, where the slope of the best fit line is $1/(K_L \times q_{max})$ and the intercept is $1/q_{max}$, as shown in Figure 4(a).

The Freundlich isotherm is a model used to describe the characteristics of adsorption on heterogeneous surfaces by multi-layer adsorption, and it assumes the presence of interaction between the adsorbent and adsorbate.The linear plot of the Freundlich isotherm model can be represented according to the Eqn. 6 (Al-Zboon *et al.*, 2011):

$$\log q_e = \mathrm{Log}\, K_F + \frac{1}{n}\log C_e \quad (3)$$

where K_F is Freundlich isotherm constant related to adsorption capacity (mg g^{-1}) and n is the heterogeneity coefficient that gives an indication of how favorable the adsorption process. When n values in the range of $n < 1$ indicate poor, $1 < n < 2$ indicates relatively difficult, and $n > 2$ indicates the good adsorption. Values of K_F and n were calculated from the intercepts (log K_F) and slopes ($1/n$) of the Freundlich plots, log q_e vs. log C_e, as shown in Figure 4(b).

Dubinin-Radushkevich (D – R) isotherm model is used to determine the distribution of Gaussian energy with an adsorption mechanism onto a heterogeneous surface, which helps to determine the adsorption mechanism and distinguish between chemical and physical adsorptions. The linear equation of this model is given by Eqn. (7) and D – R isotherm constant can be calculated using Eqn. (8) (Aljbour *et al.*, 2017):

$$\ln q_e = \ln q_s - k \times \varepsilon^2 \quad (7)$$

$$\varepsilon = RT\ln\left(1 + \frac{1}{C_e}\right) \quad (8)$$

where q_s is theoretical isotherm saturation capacity (mg g^{-1}), k is D – R isotherm constant (mol^2 kJ^{-2}), ε^2 is D – R isotherm constant, R is gas constant 8.314 (J mol^{-1} K^{-1}), T is absolute temperature at 298 K, and C_e is adsorbate equilibrium concentration (mg L^{-1}). The best fit line for experimental of adsorption of phenol using D – R isotherm model was achieved by plotting ln q_e vs. ε^2. The slope of line is k and the intercept is ln q_s, see Figure 4(c).

The adsorption energy E (kJ mol^{-1}) can be computed using the following relationship Eqn. (9):

$$E = 1/\sqrt{2k} \quad (9)$$

The adsorption energy value gives information about adsorption mechanism and more specifically its physical or chemical nature (Khan *et al.*, 2015).

Temkin isotherm model is suggested to describe the heat of adsorption of all molecules in the layer, which would decrease linearly with the increase in coverage of the active site in the adsorbent. Temkin isotherm model can be expressed by Eqn. (10) (Dad *et al.*, 2012):

$$q_e = B\ln(A_t) + B\ln(C_e) \quad (10)$$

where A_t is Temkin isotherm equilibrium binding constant (L mg^{-1}), B is constant related to heat of adsorption (J mol^{-1}). The linear fit is achieved by plotting the q_e versus ln C_e. The slope is the value of B and the intercept is A_t, see Figure 4(d).

Table 2. The parameters obtained for Langmuir, Freundlich, Temkin, and D-R isotherms for adsorption of phenol on ARH at pH=6.0, ARH dose=1.0g /1.0L, temperature= 25 °C, carbonization temperature= 550 °C, and contact time =2 h.

Parameter Model	χ^2	R^2	Parameter	value
Langmuir isotherm	1.29	0.9954	K_L (L mg^{-1})	0.062
			q_{max} (mg g^{-1})	56.8
Freundlich isotherm	-	0.9939	n	2.13
			K_F (L mg^{-1})	6.95
Temkin isotherm	-	0.9837	A_t (L m^{-1}g)	0.44
			B (J mo^{-1})	14.18
D-R isotherm	1.44	0.8422	q_s (mg g^{-1})	42.48
			k (mol^2 KJ^{-2})	0.0087
			E (kJ mo^{-1})	7.58

Table 3. The calculated parameters of pseudo-first-order, pseudo-second-order, and intraparticle models for adsorption of phenol on ARH at pH=6.0, ARH dose=1g /1.0L, temperature= 25 °C, carbonization temperature= 550 °C, and contact time =24 h.

Parameter Model	χ^2	R^2	q_{max} (mg g^{-1})	k_1(min^{-1})
Pseudo-first-order model	0.72	0.9806	40.4	0.0078
			q_{max} (mg g^{-1})	k_2 (g mg^{-1}min^{-1})
Pseudo-second-order model	0.48	0.9844	50.76	0.00026
			C (mg g^{-1})	k_i (g mg^{-1}min$^{-1/2}$)
İntraparticle model	-	0.739	0.43	2.60

The best fit model describes the adsorption isotherm and kinetic of adsorption of phenol on ARH should be associated with high correlation coefficient (R^2) and low reduced chi-square χ^2 values. The reduced chi-square is expressed by Eqn (11):

$$\chi^2 = \frac{\left(q_e^{exp} - q_e^{cal}\right)^2}{q_e^{cal}} \quad (11)$$

where q_e^{cal} is the calculated equilibrium adsorption capacity (mg^{-1}g) estimated for the isotherm models and q_e^{exp} is the experimental equilibrium adsorption capacity (mg^{-1}g) calculated using Eqn (4).

Figure 4 shows the linear plots for Langmuir, Temkin, Freundlich, and D-R isotherm models, and Table 2 provides the fitting parameters together with R^2 and χ^2 values. All results indicate that the Langmuir, Freundlich, and Temkin isotherm models are more adequate to describe the adsorption of phenol on the surface of ARH than D-R isotherm model based on the value of correlation coefficient R^2.

Langmuir, Freundlich, and Temkin isotherm models can describe the adsorption of phenol on ARH due to the presence of homogeneous and heterogeneous sites. While, the D-R isotherm model is less suitable model to describe the adsorption since the R^2 is less than 0.85.

Table 2 results indicate that the K_L value estimated from Langmuir isotherm mode is less than 1, implying that the ARH has a mono-layer coverage with a constant number of active sites, and the adsorption process is favorable. The calculated maximum q_m of Langmuir model at equilibrium situation was found to be 56.8 mg g^{-1}. According to the Freundlich isotherm model, the estimated n value was greater than 1, which reflects the favorable physical adsorption of phenol on the ARH. The adsorption energy E obtained from D-R isotherm was less than 8 kJ mol^{-1} at the studied temperature. The According to D_R isotherm, adsorption can be explained by physisorption when E is less than 8 kJ mol^{-1}, and it can be chemical adsorption when E is greater than 8 kJ mol^{-1} (Rahman *et al.*, 2017). The heat of adsorption B obtained from the Temkin isotherm has a value 14.18 J mo^{-1}. The positive value of B implies that the adsorption is endothermic and associated with a physical adsorption mechanism. These results indicate that Langmuir and Freundlich isotherm models can describe the adsorption of phenol on the ARH.

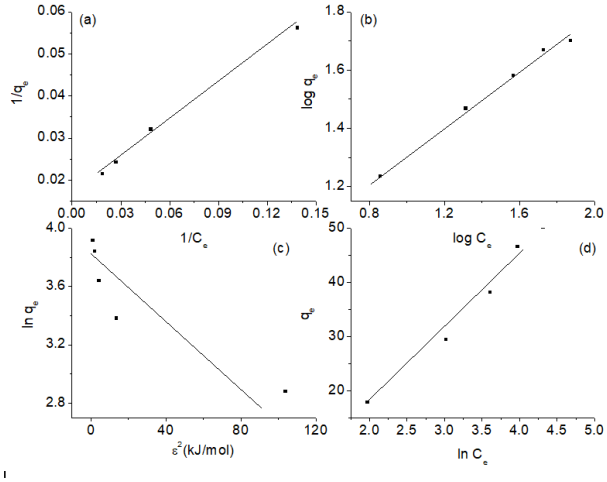

Figure 4. The linear plots of phenol onto ARH: (a) Langmuir, (b) Freundlich, and (c) D-R, and (d) Temkin at pH=6, the carbonization temperature= 550 ˚C, the contact time = 2 hrs, ARH mass=1 g/ 1L, and phenol concentration range= 25-125 mg^{-1} L

3.4. Kinetics of adsorption

Three models were used to study the kinetics of phenol adsorption onto the ARH at 25 °C. The experimental kinetic

data obtained for phenol molecules were analyzed using pseudo-first-order, pseudo-second-order, and intraparticle models (Alzboon *et al.*, 2016) (Alzboon *et al.*, 2017).

The first model is pseudo-first-order model (PFO) which was used to describes the process of adsorption by applying Eqn.(12):

$$\ln(q_e - q_t) = \ln(q_e) - k_1 t \quad (12)$$

where q_e is amount of phenol adsorbed at equilibrium (mg g^{-1}), q_t is amount of phenol adsorbed at time t (mg g^{-1}), k_1 is pseudo-first-order constant (min^{-1}), and t is time of adsorption (min).

The pseudo-second-order model (PSO) assumes that the rate of reaction depends on the quantity of solute on the surface of the adsorbent and that the rate of solute adsorption is proportional to the accessible sites on the adsorbent. The equation of this model given as in Eqn. (13):

$$\frac{t}{q_t} = \frac{1}{k_2 q_e^2} + \frac{1}{q_t} t \quad (13)$$

where q_e is amount of phenol adsorbed at equilibrium (mg g^{-1}), q_t is amount of phenol adsorbed at time t (mg g^{-1}), k_2 is pseudo-second-order constant (g mg^{-1} min^{-1}), and t is time of adsorption (min). The values of PSO rate constant and q_e were determined from the intercept and the slope of the best line of plots of t/q_e vs. t, while the slope is $1/qe$ and the intersection $1/k_2 q_e^2$.

The intraparticle model is suggested that rate limiting step in adsorption, and the adsorbate movement from the solution phase to the surface of adsorbent particles that occur in many steps. The general form of intraparticle model is given as in Eqn. (14):

$$q_t = k_i t^{0.5} + C \quad (14)$$

where q_t is amount of phenol adsorbed at time t (mg g^{-1}), k_i is interparticle constant (mg g^{-1} $min^{-0.5}$), and C is constant giving an idea about the thickness of boundary layer (mg g^{-1}).

The linear fit plots for these models are shown in Figure 5. The figures will allow estimating the calculated equilibrium adsorption capacity q_e^{cal}, k_1 is pseudo-first-order constant, k_2 is pseudo-second-order constant, the correlation coefficient R^2, and the reduced chi-square χ^2. Table provides all calculated kinetics parameters for the applied kinetics models in addition to experimental equilibrium adsorption capacity q_e^{exp}. The best kinetic model for describing phenol adsorption process should be associated with high R^2 and low χ^2values.

According to the results in Table 3 and Figure 5, the high R^2>0.98 and low χ^2 values obtained for the pseudo-second-order model kinetics model compared to the pseudo-first-order and intrapartcle models makes it suitable kinetic model for describing the mechanism of transfer the phenol from solution and controls the adsorption process on the ARH. In addition, the q_{max} (mg g^{-1}) for the pseudo-second-order model was in good agreement the q_e^{exp} value which suggests that the adsorption process of phenol on ARH is controlled by chemisorption (Rahman *et al.*, 2017).

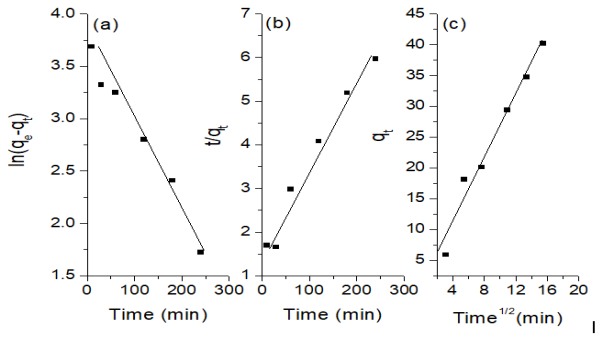

Figure 5. (a)Pseudo first order (b) Pseudo second order, and (c) Intraparticle kinetics models for the adsorption of phenol on ARH at pH=6, the carbonization temperature= 550 ˚C, the contact time = 2hrs, ARH mass=1 g/ 1L, and phenol concentration range= 25-125 mg-1 L

3.5. Thermodynamic study

Thermodynamic study is an important part to determine whether this process is favorable at elevated temperature. Adsorption thermodynamic can be expressed using the thermodynamic parameters including: standard enthalpy change ΔH° (kJ mol^{-1}), standard entropy change ΔS° (J mol^{-1} K^{-1}), and Gibbs free energy change. Thermodynamic parameters can be calculated from Eqn. (15) (Al-Zboon *et al.*, 2019):

$$\ln K_d = \frac{\Delta S^\circ}{R} - \frac{\Delta H^\circ}{RT} \quad (15)$$

where T is temperature (K), R is the gas constant (8.314 J mol^{-1} K^{-1}), K_d (mL g^{-1}) is the distribution coefficient represents the ability of the adsorbent to retain the phenol and can be calculated from Eqn. (16):

$$K_d = \frac{C_0 - C_e}{C_e \times m} \times V \quad (16)$$

where C_o is the initial concentration of phenol (mg L^{-1}), C_e is the equilibrium concentration (mg L^{-1}), V is the volume of phenol (mL), m is mass of ARH (g). The values of $\Delta H^\circ$and ΔS° were calculated from the slope ($\Delta H^\circ/R$) and intercept ($\Delta S^\circ/R$) of ln K_d versus reciprocal of temperature ($1/T$) as shown in Van´t Hoff plot, see Figure 6. The values of standard Gibbs free energy ΔG° (kJ mol^{-1}) were determined by applying the Eqn. (17):

$$\Delta G^\circ = \Delta H^\circ - T\Delta S^\circ \quad (17)$$

Thermodynamic parameters ΔH°, ΔS°, and ΔG° for the adsorption of phenol on the surface of ARH are given in Table 4**.** Data in Table 4 shows that the value of enthalpy ΔH° is positive, so the adsorption of phenol on ARH process is endothermic; the negative value for Gibbs free energy indicated that the process is spontaneous. The more negative values of the Gibbs free energy as temperature increased from 25 to 45˚C, indicate that the adsorption process on ARH was favored at high temperatures. Large value of entropy 122.3 (J mol^{-1} K^{-1}) indicates the increasing

in randomness of adsorption at the solid-liquid interface (Rahman *et al.*, 2017). This means that the adsorption occurs to phenol in the system has been successfully trapped on the surface of the ARH which is in solid phase.

Table 4. Thermodynamic parameters for the adsorption of phenol on ARH at temperature = 298.15, 308.15, and 318.15 K, pH = 6, ARH dose=1g /1.0L, carbonization temperature= 550 °C, and contact time =24 h.

Temperature (K)	ΔH° (kJ mol^{-1})	ΔS° (J mol^{-1} K^{-1})	ΔG° (kJ mol^{-1})
298.15	35.7	122.3	–0.745
308.15			–1.96
318.15			–3.19

Table 5. Removal percent of real samples.

Sample area	initial C_o (mg L^{-1})*	C_o(mg L^{-1})**	C_e (mg L^{-1})**	Removal percentage %	q_e (mg g^{-1})
Al-Kourah	1050	21	0.65	96.9%	2.035
Al-Mazar	2440	48.8	2.90	94.0%	4.59
Al-Ramtha	2925	58.5	4.0	93.1%	5.45

**Concentration of phenol in 100 mL of OMWW*

***Dilute Sample.*

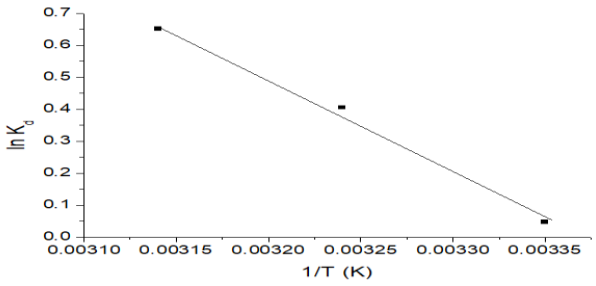

Figure 6. Van`t Hoff plot for the adsorption of phenol on ARH at pH=6, Temperature = (298-318 K), the carbonization temperature= 550 ˚C, the contact time = 24hrs, ARH mass=1 g/ 1L, and phenol concentration range= 25-125 mg-1 L

3.6. Adsorption of real OMWW samples

Olive mill wastewater contains many compounds of phenols and other pollutants. These compounds may affect the adsorption process positively or negatively. Three-real samples of OMWW from three different locations in northern part of Jordan, from the city of Irbid: (Al-Mazar, Al- Ramtha and Al-Kourah) were collected and analyzed to determine the possible impact of other pollutants on absorptive of phenol by ARH.

The polyphenols in each sample were extracted and then diluted, after that removal efficiency was determined. For 1 L of each sample with different C_0 concentrations were added to 4.0 g of ARH (produced at the optimum conditions calcium chloride at pH=6, the carbonization temperature= 850 ˚C, and the contact time = 4 hrs). The results showed that high percent removal was achieved for the sample with average removal efficiency up to 94.6% for concentration=1050 mg L^{-1} as shown in Table 5. The average adsorption capacity was 4.025 mg g^{-1}.

4. Conclusions

In this work, RH has been tested as an adsorbent to remove phenol from OMWW. RH was washed and dried then carbonized at 550 ˚C. Chemical treatment was used to produce ARH using calcium chloride. The adsorption of phenol on ARH with calcium chloride was investigated with different parameters, pH, initial concentration, dosage, contact time, and carbonization temperature. The higher percent of removal reach to 91.62 % at optimum conditions that pH= 6, phenol concentration = 50 ppm, ARH dose = 1g, contact time= 4hrs, and carbonization temperature= 850 ˚C. The ARH was characterized by Boehm titration, FT-IR, XRD, and surface area with methylene blue. Boehm titration was used to find the acidic groups on the surface of adsorbent. Most of the acidic groups were found carboxylic and phenolic with no significant of lactonic groups present. FT-IR, XRD, and the surface area of activated rice husk with calcium chloride were used and compared with known modification (phosphoric acid), the results showed that the activated carbon with phosphoric acid increased the surface area, this result supported by the FT-IR and XRD. The adsorption isotherm models fitted with Langmuir and Freundlich, the kinetic adsorption fitted with pseudo second order model, and the adsorption process is spontaneous according to the value of Gibbs free energy. Three different samples from three different places were tested; the results showed that high percentage of phenol removal was achieved with about 94.6%.

Acknowledgements

The authors would like to thank Yarmouk University - Faculty of Graduate Studies and Scientific Research for financial support. The authors would also like to thank Al-Balqa Applied University, Huson, for the facilities provided for this study.

References

Abe H. and Otsuka M. (2012). Comparison of physico-chemical characteristics among three pharmaceutical spherical carbon adsorbents. *Colloids and Surfaces B: Biointerfaces*, **100**, 90–94.

Abo Dalo D.Z. (2017). Removal of Chlorophenols from Aqueous Solutions by Adsorption on Treated Jatropha Seed Shells (Doctoral dissertation, Yarmouk University).

Al-Zboon K., Al-Harahsheh M.S., and Hani F.B. (2011). Fly ash-based geopolymer for Pb removal from aqueous solution. *Journal of hazardous materials*, **188**(1 c-3), 414-421.

Al-Zboon K., Al-Smadi B., Al-Harahsheh M. and Al-Khawaldeh S. (2019). Adsorption Modeling of Cr^{3+} on Volcanic Tuff-Based Geopolymer. *Jordan Journal of Earth and Environmental Sciences*, **10**, 35–45.

Al-Zboon K.K., Al-Smadi B.M., and Al-Khawaldh S. (2016). Natural volcanic tuff-based geopolymer for Zn removal: adsorption isotherm, kinetic, and thermodynamic study. *Water, Air and Soil Pollution*, **227**(7), 1–22.

Al-Zboon K.K., and Al-Harahsheh M.S. (2019). Adsorption of uranium on natural and thermally activated zeolitic tuff: kinetic, thermodynamic and isotherm studies. *International Journal of Environmental and Management*, **24**(1), 21–38.

Asgharnia H., Nasehinia H., Rostami R., Rahmani M. and Mehdinia S.M. (2019). Phenol removal from aqueous solution using silica and activated carbon derived from rice husk. *Water Practice and Technology*, **14**(4), 897–907.

Dada A.O., Olalekan A.P., Olatunya A.M. and Dada O.J.I.J.C. (2012). Langmuir, Freundlich, Temkin and Dubinin-Radushkevich isotherms of equilibrium sorption of Zn+2 unto phosphoric acid modified rice husk. *IOSR Journal of Applied Chemistry*, **3**(1), 38–45.

Daffalla S.B., Mukhtar H. and Shaharun M.S. (2010). Characterization of adsorbent developed from rice husk: effect of surface functional group on phenol adsorption. *Journal of Applied Sciences*, **10**(12), 50–58.

Daraei H., Noorisepehr M., Kamali H. and Daraei F. (2014). Efficiency of eggshell membrane in removal of phenol from aqueous solution. *Journal of health and hygiene*, **5**(1), 7–17.

Della Greca M., Monaco P., Pinto G., Pollio A, Previtera L. and Temussi F. (2001). Phytotoxicity of low-Molecular-Weight phenols from olive mill waste waters. *Bulletin of environmental contamination and toxicology*, **67**(3), 352–359.

Dursun G., Cicek H. and Dursun A.Y. (2005). Adsorption of phenol from aqueous solution by using carbonized beet pulp. *Journal of hazardous materials*, **125**(1–3), 175–182

Ghasemi Z., and Younesi H. (2011). Preparation and characterization of nanozeolite NaA from rice husk at room temperature without organic additives. *Journal of Nanomaterials*, **2011**, 1–8.

Goertzen S.L., Theriault K.D., Oickle A.M., Tarasuk A.C. and Andreas H.A. (2010). Standardization of the Boehm titration. Part I. CO_2 expulsion and end point determination. *Carbon*, **48**(4), 1252–1261.

Kajjumba G.W., Emik S., Öngen A., Ozcan H.K., and Aydin S. (2018). Modelling of Adsorption Kinetic Processes—Errors, Theory and Application. In: Advanced sorption process applications, Editor: Edebali S., IntechOpen, London.

Kavitha D. (2016). Adsorptive removal of phenol by thermally modified activated carbon: Equilibrium, kinetics and thermodynamics. *Journal of Environment & Biotechnology Research*, **3**(1), 24–34

Khalid N., Ahmad S., Toheed A. and Ahmad J. (2000). Potential of rice huskes for antimony removal. *Applied Radiation and Isotopes*, **52**(1), 31–38

Khan T.A., Khan E.A., and Shahjahan. (2015). Removal of basic dyes from aqueous solution by adsorption onto binary iron manganese oxide coated kaolinite: non-linear isotherm and kinetics modeling. *Applied Clay Science*, **107**, 70–77.

Kioni P.N., Gao Y., Tang Z., Gatebe E. and Wanyika H. (2011). Synthesis and characterization of ordered mesoporous silica nanoparticles with tunable physical properties by varying molar composition of reagents. *African Journal of pharmacy and Pharmacology*, **41**(89), 227–156.

Lopez-Ramon M.V., Stoeckli F., Moreno- Castilla C. and Carrasco-Marin F. (1999). On the characterization of acidic and basic surface sites on carbons by various techniques. *Carbon*, **37**(8), 1215–1221.

Michalowicz B. (2006). Adsorption and desorption of phenol on activated carbon and a comparison of isotherm models. *Journal of hazardous materials*, **129**(1–3), 158–163.

Michalowicz J. and Duda W. (2007). Phenols – Sources and Toxicity. *Polish Journal of Environmental Studies*, **16**(3), 347–362.

Nasif M., Adnan A.L.A. and Saaed A.L.F. (2013). Phenol removal from wastewater using rice husk. *Diyala Journal for Pure Science*, **9**(4), 64–77.

Pajooheshfar S.P. and Saeedi M. (2009). Adsorptive removal of phenol from contaminated water and wastewater by activated carbon, almond, and walnut shells charcoal. *Water environment research*, **81**(6), 641–648.

Pelekani C. and Snoeyink V.L. (2000). Competitive adsorption between atrazine and methylene blue on activated carbon: the importance of pore size distribution. *Carbon*, **38**(10), 1423–1436.

Pirzdeh K. and Ghoreyshi A.A. (2014). Phenol removal from aqueous phase by adsorption on activated carbon prepared from paper mill sludge. *Desalination and water treatment*, **52**, (34–36), 6505–6518.

Rahmanian N., Jafari S.M. and Galanakis C.M. (2014). Recovery and removal of phenolic compounds from olive mill wastewater. *Journal of the American Oil Chemists Society*, **91**(1), 1–18.

Sahu O., Rao D.G., Gabbiye N., Engidayehu A. and Teshale F. (2017). Sorption of phenol from synthetic aqueous solution by activated saw dust: Optimizing parameters with response surface methodology. *Biochemistry and biophysics reports*, **12**, 46–53.

Sarker N. and Fakhruddin A.N.M. (2017). Removal of phenol from aqueous solution using rice straw as adsorbent. *Applied Water Science*, **7**(3), 1459–1465.

Sayed M.S. (2008). International Conference for Nuclear Sciences and Applications, Sharm Al Sheikh (Egypt), 11-14 Feb 2008; Related Information: In: Proceedings of the 9. International Conference for Nuclear Sciences and Applications, 1239 pages.

Yin C.Y., Aroua M.K. and Daud W.M.A.W. (2007). Review of modifications of activated carbon for enhancing contaminant uptakes from aqueous solutions. *Separation and purification technology*, **52**(3), 403–415.

Zanella O., Tessaro I.C., and Feris L.A. (2014). Study of $CaCl_2$ an agent that modified the surface of activated carbon used in sorption treatment cycles for nitrate removal, *Brazilian Journal of chemical Engineering*, **31**, 205–210.